Journal of Hydrology 565 (2018) 331–340

Contents lists available at ScienceDirect

Journal of Hydrology

journal homepage: www.elsevier.com/locate/jhydrol

Research papers

Use of sodium fluorescein dye to visualize the vaporization plane within porous media

Tomáš Weiss, Martin Slavík*, Jiří Bruthans

Faculty of Science, Charles University, Albertov 6, 128 43 Prague 2, Czech Republic

ARTICLE INFO

This manuscript was handled by C. Corradini, Editor-in-Chief, with the assistance of Juan V. Giraldez, Associate Editor

Keywords:
Evaporation
Capillary water
Drying front
Evaporation front
Capillary zone
Dry surface layer

ABSTRACT

The vaporization plane in porous media separates the region of capillary flow from the dry surface layer, where the water transports only in its gas phase. Knowledge of the depth and geometry of the vaporization plane is critical for estimating water flux in the soil-atmosphere interphase, for understanding evaporating processes in general, and for prediction of locations of damaging salt crystallization, etc. However, detection of the vaporization plane is a challenging task. This paper explores the use of sodium fluorescein dye (uranine), a popular hydrological tracer, to visualize the vaporization plane in porous media. Uranine was used in the forms of solution or powder on sand, sandstone, and autoclaved aerated concrete, in both laboratory and field experiments. The property of uranine solution to change its color according to its concentration can be used to: i) visualize the vaporization plane by forming a distinctive dark-orange zone where the pore water evaporates, and ii) to distinguish the zone of vapor flow from the zone where capillary flow is present. Similarly, uranine powder, when applied onto a porous material, clearly visualizes the dry surface layer and the capillary zone, divided by the vaporization plane. This technique can also visualize a complex-shaped vaporization plane in hydrophobic materials. In comparison with other techniques, such as sensible heat balance or heat pulse methods, the use of uranine is accurate, cost-effective, and straightforward.

1. Introduction

Evaporation is a key process in the land-atmosphere water balance; additionally, the near-surface flow in porous media is an important topic for natural and engineering sciences such as agriculture, soil science, hydrology, or studies of rock weathering, building structures decay, or endolithic biology. Evaporation from coarse porous media can be conceptually divided into three stages (Idso et al., 1974; Hillel, 2004; Or et al., 2013). In the third stage, a critical suction is reached in the subsurface, and the so-called vaporization plane (VP) is formed, separating the region of the capillary zone (CZ) with its capillary flow from the dry surface layer (DSL), where water flows only in the gas phase (Shokri et al., 2009; McAllister et al., 2016). In the CZ, where saturation is above the critical suction, water flows via a network of partly saturated pores due to the pressure head gradient, and its flow is usually described by Richards (1931) equation. In the DSL, the water vapor movement is conceptually given by Fick's Law (Bittelli et al., 2008). Knowledge of the DSL thickness and the geometry of the VP are critical for estimating the water flux in the soil-atmosphere interface, and thus for understanding evaporation processes in general (Shokri and Or, 2011; Bruthans et al., 2018).

An understanding of moisture dynamics in porous media is also crucial for the prediction of material decay for both building structures and natural outcrops (Fidríková et al., 2013; Mol and Viles, 2013). Water represents one of the main degradation factors, capable of seriously reducing the durability of materials (Falchi et al., 2015), as well as being one of the most critical factors facilitating the growth of mold and microbes that can pose health hazards to people (Viitanen et al., 2010). Detection of the VP is particularly important in studying a material's decay by salt weathering. As dissolved salts are transported by the capillary water, and precipitated within the material, they form crystals (Huinink et al., 2004), with the resulting increased pressure caused by the crystallization leading to the material damage (Rijniers et al., 2005). Therefore, the location of salt crystallization in the VP is closely related to material decay. Detection of the VP could also potentially be used in the soil science of (semi-)arid regions, where salinization of the soil is an important issue, and an understanding of salt accumulation can lead to better agriculture practices (Kurtzman et al., 2016).

The VP can be located by several direct and indirect methods (see

Abbreviations: VP, vaporization plane; DSL, dry surface layer; CZ, capillary zone; BB, Brilliant Blue; AA, autoclaved aerated

* Corresponding author.
E-mail address: slavikma@natur.cuni.cz (M. Slavík).

https://doi.org/10.1016/j.jhydrol.2018.08.028
Received 27 May 2018; Received in revised form 3 August 2018; Accepted 12 August 2018
Available online 14 August 2018

Table 1 in Suppl. mat.). As heat balance is an important factor controlling evaporation (Gupta, 1974; Mikhailov, 1975), heat-pulse or sensible heat balance methods can be used for its determination (Trautz et al., 2014). These heat-based methods are limited by needle spacing, and they are required to be installed at precisely defined depth intervals (Xiao et al., 2012). The VP can also be found by measuring the water content. These methods are easy-to-employ and inexpensive. The electric- and magnetic-based methods are either not accurate enough (time domain reflectometry method; Topp et al., 1982) or they are influenced by the amount of dissolved solids (protimeters; Mol and Viles, 2010). Identification of the VP is usually not possible by measuring the pressure head with tensiometers, as the suction is out of measuring limits. More demanding methods include nuclear magnetic resonance imaging (Reis et al., 2003; Sněhota et al., 2010; Lehoux et al., 2016), X-ray tomography (Rad et al., 2015), acoustic emission (Grapsas and Shokri, 2014), neutron radiography (Deinert et al., 2004; Sacha et al., 2015), confocal microscopy (Xu et al., 2008), gamma ray densitometry (Shahidzadeh-Bonn et al., 2007), and electrical resistivity tomography (Daily et al., 1992; Mol and Viles, 2010).

The techniques used for detection of the VP within porous media require either special devices and/or have a low spatial resolution (for details about the methods and their limits, see Table 1 in Suppl. mat.). An easy-to-use and cost-effective method with good resolution has, to date, been lacking in hydrological science. The use of dyes is an attainable means to tackle the disadvantages of the methods mentioned above. In several evaporation studies, Brilliant Blue FCF dye tracer has been used to visualize the VP (Lehmann and Or, 2009; Shokri et al, 2009). However, this has been found unsuitable for tracing the travel time of water, because of its sorption properties (Kasteel et al., 2002). Concerning other uses of dyes, uranine (sodium fluorescein) dye has recently been used to visualize the complex pattern of hydrophobicity in the biologically-initiated rock crust on sandstones (Slavík et al., 2017), and even the VP within sandstone (Bruthans et al., 2018).

The aim of this study was to test the use of uranine dye in solution and powder forms to visualize the VP, CZ, and DSL in porous media. The following steps were taken to reach the aim, that is, to test if this new method is viable in different porous media and under various boundary conditions:

- In the first step, we tested *dissolved* uranine dye to visualize the VP, CZ, and DSL zones in sand, sandstone and autoclaved concrete as examples of common natural and building materials. Correct distinction of the zones was verified by testing the material cohesion, and by examining the presence of liquid water by a microscope. At first, tests were done under semi-steady state of VP, CZ, and DSL location, later under transient conditions (increased water supply from below or increased potential evaporation resulting in migration of the zones). To test if the technique can trace former distribution of VP, CZ, and DSL in already dried material, specimens with uranine solution were dried completely and subsequently cut and inspected. Finally, the technique was tested on sandstone samples with hydrophobic layer, i.e. in complex environment in terms of capillary flow.
- In the second step, we compared the uranine and Brilliant Blue dyes' ability to visualize the VP, CZ, and DSL in sand.
- In the third step, uranine in the form of *powder* was tested in lab and field experiments to visualize the three zones in sandstone.
- Finally, the applicability of the method using uranine solution or powder, comparison with other methods, and the need for future development of the proposed technique was discussed.

2. Materials and methods

2.1. Materials

2.1.1. Dyes

In the experiments presented herein, we have used mainly uranine dye ($C_{20}H_{10}Na_2O_5$), and, in one experiment, Brilliant Blue FCF dye (hereafter BB; both obtained from Sigma Aldrich in powder form). Uranine is a dark red powder when dry, and the color of a uranine-water solution changes (with decreasing concentration) from red to orange to yellow and finally to light green (Käss, 1998; Fig. 1 in Suppl. mat.). Uranine, unlike BB, has the ability to fluoresce (i.e., adsorb shorter wavelength light and emit at a longer wavelength) at lower concentrations. BB is always blue in color: dark blue in dry powder form and lighter blue in water solution.

Uranine, discovered in 1871, is a manufactured organic compound usually used as a dye, with numerous applications ranging from medicinal use (Can Med Assoc J, 1959; Mathew, 2014) to forensics (Budowle et al., 2000), and cosmetics. In the natural sciences, uranine is used in biochemical research as a common fluorophore in microscopy (Lakowicz, 2006), and as a fluorescent probe in cytogenetic techniques (Noga and Udomkusonsri, 2002). In the earth sciences, uranine is used as a rather conservative tracer in tracer tests and for the visualization of the preferential pathway(s) of groundwater flow for its relatively low-reactive (low-sorbing) properties in comparison with other organic dyes (Gaspar, 1987; Wilson et al., 2016), even though sorption was observed to be significant on soils (Gerke et al., 2008). For a summary of the available literature on uranine's main physical and chemical properties see Gerke et al. (2013). BB is an organic compound, which besides being a food coloring, is often used as a tracer in soil-profile scale studies for the visualization of flow pathways in soils (e.g., Kasteel et al., 2002). Of the non-fluorescent tracers, Flury and Flühler (1995) concluded BB to be the best tracer to use because of its mobility, visibility, and low toxicity. For BB's main physical and chemical properties see Flury and Flühler (1995).

Sorption characteristics of the dyes are important for migration of dye solutions in capillary form. There are several adsorption studies of BB (e.g., Ketelsen and Meyer-Windel, 1999; Germán-Heins and Flury, 2000; Kasteel et al., 2002; Mon et al., 2006; Morris et al., 2008) and uranine (e.g., Smart and Laidlaw, 1977; Sabatini and Austin, 1991; Kasnavia et al., 1999; Sabatini, 2000; Gerke et al., 2008; Gerke et al., 2015). However, as these studies were done for different types of soils and under different settings, comparisons of these findings and predictions of a tracer's behavior in a particular experiment is difficult. Even though there is a study comparing the two dyes in their ability to stain preferential pathways (Vlček et al., 2017), to the best of our knowledge, there has never been a study purposefully comparing sorption under neutral pH of the two dyes in the same material. Nevertheless, based on the literature reviewed, we expect BB to sorb more than uranine. The basic properties of uranine and BB are shown in Table 1.

Table 1
Selected physical and chemical properties of uranine and BB (Brilliant Blue FCF).

Property	Uranine	Brilliant Blue FCF	Reference
Chemical formula	$C_{20}H_{10}Na_2O_5$	$C_{37}H_{34}N_2Na_2O_9S_3$	–
CAS number	518-47-8	3844-45-9	–
Molar mass (g/mol)	378.28	792.85	–
Color Index	C. I. 45 350; Acid Yellow 73	C. I. 42 090; Acid Blue 9, Food Blue 2	(CI, 2001)
Solubility in water	> 600 g/l	200 g/l	(Käss, 1998; Marmion, 1991

2.1.2. Porous materials

To test if the technique is applicable for various porous materials, several common natural and building materials were used: sand, sandstone, sandstone with natural hydrophobic layer, and autoclaved aerated (AA) concrete. The sand and gravel (the later used as a drain in a bottom of experimental setup only) used in the experiments were from the Kaznejov quarry (Czech Rep.). Certified sieves were used to determine the grain sizes of the loose materials (both dominating in quartz): 0.2–2 mm for the sand, and 2–4 mm for the gravel. The sandstone used (both with and without the hydrophobic layer) was a medium-fine grained quartz sandstone from the Bohemian Cretaceous Basin (Czech Rep.) with grain sizes from 0.25 to 0.5 mm (for details see Bruthans et al., 2018). We used AA concrete with the commercial name Ytong P2-500, having a dry bulk density of 475 ± 25 kg/m^3 and pore diameters < 3.5 mm. Field observations were done at the exposures of fine to coarse grained quartz sandstone from the Bohemian Cretaceous Basin (Czech Rep.), 60–70 km NE from Prague. Further details about the materials used are given in Table 2 in Suppl. mat.

2.2. Methods

Porosity of the compact materials used was measured by high-pressure mercury porosimetry using an AutoPore IV 9520 instrument (Micromeritics, USA) and the skeletal (true) density, ρHe, was determined by means of a gas pycnometer instrument. For more details see Supplementary material by Slavík et al. (2017). Porosity of the sand was calculated from the dry bulk density (dried in an oven at 105 °C for 24 hrs) of the sample with known volume.

Capillary water absorption (CWA) of cores of the compact materials was measured using a Sauter FH 50 N tensiometer (d = 0.01 N, capacity 50 N). The bottom base of the core was put in contact with the water surface, and the weight of the core was recorded at one second intervals until the maximum moisture content was reached by capillary uptake. Decrease of the water level during measurement was negligible (< 1 mm). The CWA was calculated as the weight of water absorbed per unit area per unit of time (gm^{-2}s^{-1}).

Potential evaporation was measured gravimetrically by evaporation of water from PVC cups (diameter 103 mm, height 395 mm). There were three cups in the laboratory environment, two of which had controlled wind speed at the cup surface (2.5 ± 0.5 m/s and 1.0 ± 0.3 m/s), and the last was in the environment with ambient air motion. The water table was kept between 5 and 15 mm from the top of the cups.

A portable digital Levenhuk DTX 500 Mobi microscope (magnification 20-200) was used to obtain detailed visualization of the uranine solution in the pore space. The wind speeds were measured with thermal anemometer - Model TA 410 XY Airflow by Greisinger electronic GmbH. All experiments were photo-documented.

2.3. Experimental setup

We carried out both laboratory and field experiments. The design of the presented experiments and the solution concentrations used are based on several preliminary experiments and here we show only the final experimental setups which are demonstrating specific settings of boundary (initial) conditions. The results of the preliminary experiments nevertheless fully correspond to the results presented in this paper. The uranine and BB dyes were applied in the form of water solutions, which were prepared (in the lab) by dissolving the respective dye powder in distilled water (concentrations are given below and in Table 2 in Suppl. mat.). Uranine was also used in the form of a dry powder (both in the lab and the field). In all the laboratory experiments, ambient temperature and relative humidity of the air and/or potential evaporation were measured. For overview on all tests and further specifications concerning individual experiments, see Table 2 and Fig. 2 in Suppl. mat.

2.3.1. Experiments with dye solutions

The porous material was first dried in the laboratory environment (19–21 °C, 35–40% relative humidity) until no change in sample weight occurred within a 24 hrs interval. There were three reasons for this experimental setting: (i) For the samples to be in equilibrium with the surrounding environment to eliminate any uncontrolled moisture uptake from the water vapor in laboratory atmosphere, (ii) to reach more or less the same moisture of all the samples, and (iii) because the organisms colonizing the sandstone core in exp. 1e (see further) would not survive oven drying.

Unless stated otherwise, the experiments were carried out in the same laboratory environment. To ensure homogenization of the sand and its minimal compaction, the material was carefully placed into glass containers while being continuously mixed with a metal rod. Changes in the color of the samples resulting from the solution's transport were photo-documented. The samples were saturated via the entire bottom boundary with dye solutions. This approach was chosen for four reasons: (i) in order to make the experiments more rapid (in case of full saturation and subsequent drying, the experiment would take longer time), (ii) it enables uniform absorption of solution via the respected surface area and its more or less uniform movement throughout the sample, and (iii) this setting helps in clear visual distinction of the three zones – if we first saturated the sample and let it evaporate, there would be uranine precipitated in the DSL and thus the VP would not be seen as a visually distinctive line, and (iv) saturation via a bottom boundary and evaporation via upper boundary replicates moisture distribution in many natural settings (e.g. Bruthans et al., 2018).

Concerning the volumes of dye solutions injected, we used just enough solution for the VP to form inside a sample, that is, to form the three zones in a sample at the same time: DSL, VP, and CZ. By injecting the limited volume of solution, we avoided CZ to rise by capillary forces all the way up to the surface.

2.3.1.1. Experiment 1a. This experiment was conducted to test if dissolved uranine dye correctly visualizes the VP, CZ, and DSL in sand. A glass container (7 × 15 × 15 cm), sealed from all sides except the top boundary where evaporation took place, was uniformly filled with sand above a 1 cm thick basal layer of gravel serving as a drain that helped to redistribute the injected solution. In the middle of the container, a plastic tube was vertically placed to enable injection of the solution into the gravel at the bottom. The experiment was carried out under a constant wind speed condition (1.0 ± 0.3 m/s) maintained by an electrical fan at the top boundary. Uranine solution (2 g/l) was injected through the plastic tube into the gravel (90 ml, one time only). After the injection, the plastic tube was plugged with a plastic stopper to avoid evaporation from the drain. After the experiment and documentation of VP by uranine's color, the containers were tilted > 45° to separate the dry (loose) sand from wet (capillary held) sand to verify the VP position. For details see Fig. 2 in Suppl. mat.

2.3.1.2. Experiment 1b. This experiment was performed to test if dissolved uranine dye visualizes the VP, CZ, and DSL in compact materials. A sandstone core and an AA concrete core (~50 mm thick, ~70 mm in diameter) were placed into two PVC cups closed all around except the top boundaries to avoid evaporation from the cores' sides and bottoms. Uranine solution (1.3–3 g/l; 20–30 ml; for details see Table 2 in Suppl. mat.) was injected into the bottom (one time only) of the cups making sure that it is absorbed by the sample through its bottom boundary only.

2.3.1.3. Experiment 1c. To test if the zones are traceable under transient conditions (increased water supply from below or increased potential evaporation resulting in migration of the zones), experiment 1c was carried out using the same experimental settings as exp. 1a using two glass containers (7 × 15 × 15 cm). Wind speed conditions were

controlled throughout the experiment maintained by electrical fans to sustain the desired potential evaporation. In both containers under wind speed of 1 ± 0.3 m/s, uranine solution (2 g/l) was injected through the plastic tubes into the gravel (90 ml), which were plugged by stoppers after the injection. Once the solution stopped moving upwards (7 days), the two containers were treated in different ways:

In the first container, windspeed of the fan was increased to 2.5 ± 0.5 m/s to push the VP down. After the documentation of the VP by uranine's color, the container was tilted > 45° to verify the VP position (see exp. 1a for reasoning).

In the second container, more uranine solution was injected to the bottom (120 ml, 2 g/l) to push the VP further up. After the solution stopped moving upwards (after another XX days), it was photo-documented, and the container was tilted to verify the VP position.

2.3.1.4. Experiment 1d. To test if the technique can trace former distribution of VP, CZ, and DSL in already dried material, a sandstone core (~50 mm thick, 70 mm in diameter) was placed into an open plastic container (enabling evaporation from all the sides except the bottom) filled with a 2 cm layer of uranine solution at its base (2.6 g/l). The uranine solution moved upwards due to capillary uptake. The core was periodically weighted (1–2 days), and after three weeks, when the material had dried (no measurable change in sample weight during 24hrs occurred), the sample was cut in half, photo-documented, and subsequently the cut surface was made wet by < 1 ml of distilled water to partly remobilize the precipitated uranine and in 15 min photo-documented again.

2.3.1.5. Experiment 1e. To test the uranine solution on materials with uneven capillary flow and complex VP geometry, a sandstone core was used (~50 mm thick, ~70 mm in diameter) with naturally developed biologically-initiated rock crust consisting of hydrophobic organic matter (for details see Slavík et al., 2017 who studied the same material) on its upper base of uneven surface. The core was placed into a PVC cup like in exp. 1b and uranine was repeatedly added into the bottom of the cup (1.3 g/l, see Table 3 in Suppl. mat.). A sandstone core of the same size and under the same experimental settings but without crust was used for comparison. At the sandstone core's upper base, a pit (20 mm deep and 30 mm in diameter) was hollowed out to (i) enable comparison with the similar surface of the sample with the crust, (ii) to observe dye precipitation once water reaches the surface, (iii) to test whether the solution is moving uniformly throughout the core. The weight of the cores was monitored.

2.3.1.6. Experiment 2. In experiment 2, we compared the effectiveness of the uranine and BB dye solutions to visualize the VP, CZ, and DSL in sand. BB dye had been already used in evaporation studies (e.g. Lehmann and Or, 2009; Shokri et al., 2009). Two 400 ml glass beakers were uniformly packed with sand. Into one, 10 ml of 1.3 g/l uranine solution was injected; 10 ml of 0.4 g/l BB solution was injected into the other beaker. Concentrations of both dyes were determined from preliminary tests to ensure ideal visibility. Both injections were performed by a medical needle that run via the middle of the sample to the very bottom. The samples were left in the laboratory environment to evaporate for 18 hrs. After the experiment and documentation of VP by uranine's color, the containers were tilted > 45° to verify the VP position (see exp. 1a for reasoning).

2.3.2. Experiments with uranine powder

2.3.2.1. Experiment 3a. The laboratory experiment 3a was testing uranine powder to visualize the VP, CZ and DSL zones in sandstone. A sandstone core (~50 mm thick, ~70 mm in diameter) was placed into an open plastic container filled with 2 cm of water at its base. After 5 min, the core was taken out of the water and uranine powder was dusted onto the sandstone core's surface using a makeup brush; after 2 min it was photo-documented.

2.3.2.2. Experiment 3b. In the field, holes were drilled (80 mm diameter, ~60 mm depth) with a core drill bit into the natural sandstone body perpendicular to the rock surface (in various directions from vertical to horizontal). Drilling was done without the use of water or air flushing to avoid wetting or drying of the environment. Drilling took several tens of seconds and care was taken not to heat the drill bit considerably (to avoid evaporation). Once the drilling was finished, uranine powder was immediately applied onto the sides of the drilled hole, and onto the surrounding surface of the sandstone by dusting the powder using a makeup brush; after 5 min it was photo-documented.

3. Results and discussion

3.1. Experiments with uranine dye solution

In the evaporation experiments, we injected uranine solution into the bottom of both loose and compact materials, and let the solution evaporate in porous media. In all cases, we observed (after several hours-days) that the uranine solution forms two differently colored zones in porous media: (1) a yellow color zone, and (2) a distinctive dark-orange zone (Fig. 1). The yellow color zone (1) was colored by the solution, and therefore represents the volume where uranine was carried by liquid water. This flow is presumably due to capillary forces, and hereafter we call (1) the capillary zone (CZ). On the contrary, the dark-orange color (2) is a consequence of increased uranine concentration (Käss, 1998), which can only be explained by evaporation within the media. If the solution in the CZ was adsorbed to the material's particles, we would see a gradual color change, as adsorption increases with solution concentration (Appelo and Postma, 2013). Therefore, the increased uranine concentration clearly indicates evaporation within the porous material – the vaporization plane (VP), dividing the CZ below from the dry surface layer (DSL) above (Fig. 1). We hence state that the yellow color zone represents the CZ, the dark-orange zone stands for the VP, and the non-colored area points to the DSL

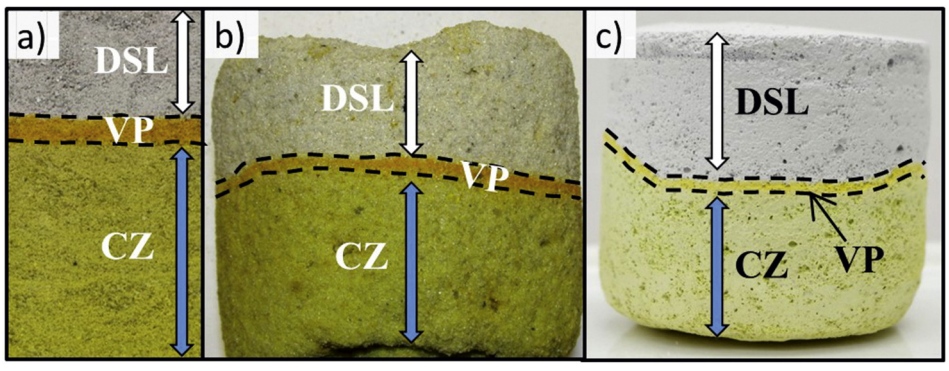

Fig. 1. Examples from experiments with a) loose sand (exp. 1a), b) sandstone core (exp. 1b), and c) AA concrete core (exp. 1b). In all experiments, three differently colored zones were observed: (1) a yellow colored zone of capillary flow (CZ), (2) a distinctive dark-orange zone, visualizing the plane of evaporation (VP), and (3) a dry area not colored by uranine (DSL). (For interpretation of the references to color in this figure legend, the reader is referred to the web version of this article.)

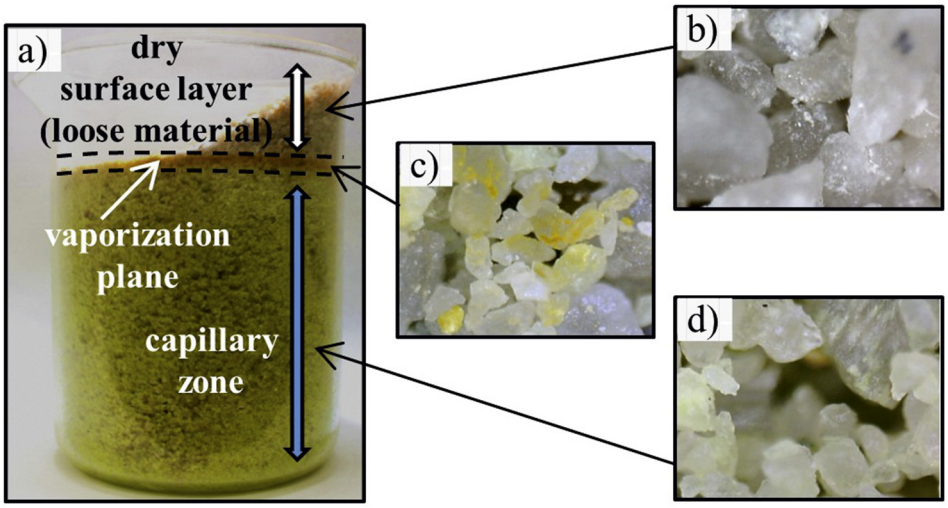

Fig. 2. Experiment 2 proving the presence of the DSL zone. a) Uranine solution was moving upwards by capillary forces in the glass container, and after 18 h, the VP was observed close to the surface. After tilting the glass container by 45°, the sand grains in the DSL, which were loose, moved freely as no cohesive forces were present; while the wet part (CZ) stayed intact due to cohesion by capillary forces. These two parts (DSL and CZ) were divided by a thin VP. The sand particles in the three zones were observed under a microscope: b) for DSL, c) for VP, and d) for CZ. Since the microscope camera automatically adapts the color spectrum to the actual composition, the particles from the CZ (d) appeared only slightly yellow in the photo, even though the yellow color was clearly visible in the microscope before the automatic color spectrum adjustment. (For interpretation of the references to color in this figure legend, the reader is referred to the web version of this article.)

(where water moves in the form of vapor only, and thus not transporting any dye).

To further prove that the yellow zone is equivalent to the CZ, and the non-colored zone equivalent to the DSL, we checked the presence of water cohesion forces by tilting the glass container after experiment (exp. 2) with sand at an angle of 45°. The particles above the VP were loose and separated from the rest of the material (Fig. 2). This demonstrated the lack of cohesion forces in the DSL, as capillary menisci were not present in the dry medium. Note that the described drying process (change in VP location) is slow and that any measurable change takes hours, therefore seconds-long tilting of the container does not change the location of the VP. To further identify the differences between the three zones, we used a microscope. Below the VP, the particles appeared shiny, as water formed very thin films (Fig. 2b). At the VP, one could distinguish some particles being covered with uranine solution films of a dark-orange color (Fig. 2c). Above the VP, the sand particles appeared dim and dry, partly covered with what appears to be fines disintegrated from the particles (Fig. 2d).

The spatial distribution of the dark-orange zone and the yellow zone can change over time, which could be due to e.g., an increased water supply below the VP or an increased potential evaporation above the VP. There are two basic scenarios: either the VP moves toward the surface - progresses (Fig. 3a) or it retreats into the material (Fig. 3b). In the first scenario, the observed color correctly reflects the current situation as the uranine solution moves to the previously dry (not colored) portions, and the former dark-orange zone of the VP dissolves into the advancing capillary solution. Still, remnants of the former VP may be visible in the CZ, especially if the former VP was stabilized for a longer time. In the second case, when the CZ shrinks, and the DSL expands into the region formerly occupied by CZ, the dark-orange zone either thickens and/or several dark-orange strips are formed below the former VP (Fig. 3b). In this case, the actual VP is represented by the lowest dark-orange strip, while the other dark-orange strips are remnants of the retreating VP (this was tested by tilting the samples). To summarize, uranine can partly overprint previous stages of moisture distribution; however, in the case of drying, it is necessary to interpret the dark-orange zone in the context of its former positions and the change of conditions. Uranine solution can thus reveal some information about the evolution of the moisture system – whether the CZ was retreating or progressing towards the surface.

In all the cases presented above, the CZ was observed while the sample was still wet (see Table 2 in Suppl. mat.). In some cases, it can be advantageous to observe the results of the experiment after a complete drying of the sample, so that the CZ and VP are not present in the sample anymore. The former spatial distributions of the CZ and VP can

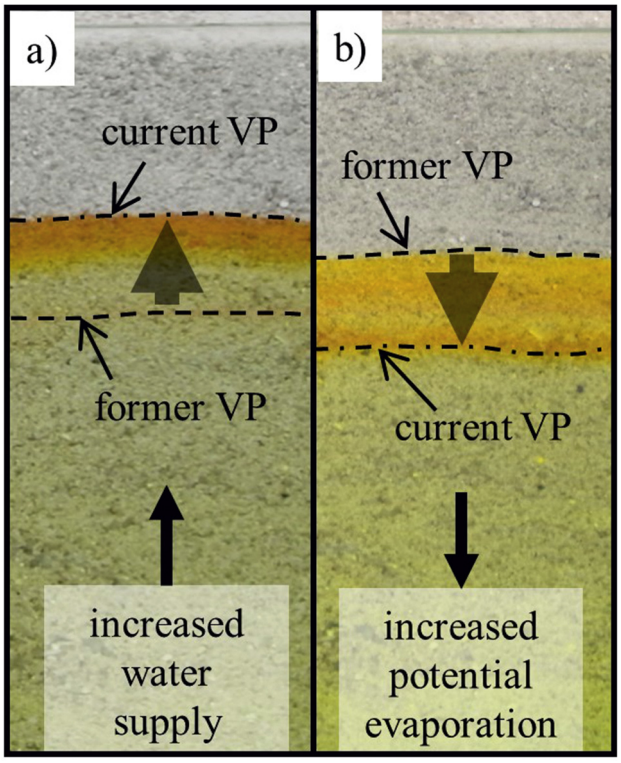

Fig. 3. Uranine visualization of changes of the spatial distribution of the CZ, VP, and DSL in exp. 1c. a) The VP has moved upwards towards the surface (progressed) due to increased capillary water supply from below. The former VP is hardly visible as it has dissolved in the moving solution. b) The VP has moved downwards (retreated) due to increased potential evaporation. The current VP is represented by the lowermost of all the dark-orange strips. (For interpretation of the references to color in this figure legend, the reader is referred to the web version of this article.)

still be imprinted into the material. In particular, clear visualization of the former CZ and VP occurs if the VP is present at a constant depth for a relatively long time. This is the case documented in Fig. 4a, where the entire sandstone core was initially wet through its bottom with uranine solution; subsequently, it was allowed to evaporate in an open environment until it became completely dry (until the weight of the sample was in steady state), and then was cut in half. Because of the high initial saturation of the sample and the relatively fast evaporation, the VP was thus at the very surface of the sample during most of the

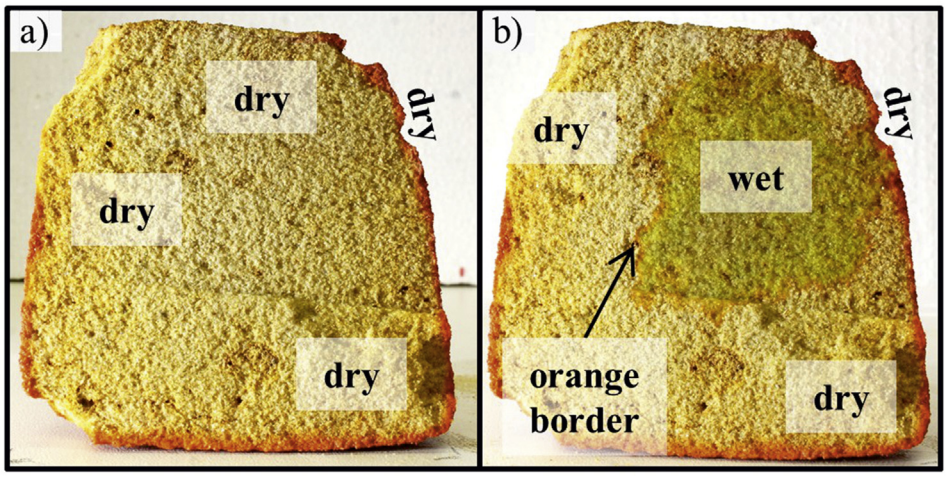

Fig. 4. Experiment 1d showing dry sample cut in half after relatively fast evaporation. a) The sandstone core sucked up the uranine solution and evaporated via its entire surface. After some time, the uranine solution supply stopped, and since then, no additive capillary water has been injected into the core and the core was drying. After complete drying, the sandstone core was cut in the middle. Visualization of the former spatial distribution of the CZ and VP from the time when the uranine supply stopped was imprinted in the sandstone core. b) After complete drying of the core, distilled water was injected onto the cut dry surface. The distilled water was spreading sideways, while dissolving the precipitated uranine, and the boundaries of the wet zone continuously changed its color from yellow to light orange. (For interpretation of the references to color in this figure legend, the reader is referred to the web version of this article.)

drying process, and hence the imprinting of the CZ (yellow zone), and the VP (dark-orange zone) close to the surface. However, when the VP changed its position relatively quickly, its imprinting into the material was not apparent (the inside of the core in Fig. 4a) or was limited (variously colored zone between the former and current VPs in Fig. 3b).

When using a material with some precipitated uranine already present, the observations should also be interpreted with caution, as this influences the resulting color. This is visible from Fig. 4b, where after wetting the cut dry surface with drops of distilled water, a new spatially limited area of capillary water was established. As the distilled water was spreading sideways, and thus dissolving the precipitated uranine in the material along the way, the boundaries of the wet zone continuously changed its color from yellow to light orange. Therefore, only the border of the area of this water spread was forming a distinctive light orange line, even though evaporation must have taken place from the entire area wetted by the distilled water (see Fig. 4b).

We tested whether it is possible to visualize the VP in the special case of a sandstone core with a hydrophobic layer. Uranine visualized that the hydrophobic layer at the top of the core (a few mm thick, Slavík et al., 2017) hindered the upward movement of the solution, so that the capillary flow was not permitted to reach the very top of the core, resulting in an uneven geometry of the VP (Fig. 5a). In comparison, in the same sandstone material, except without the hydrophobic layer, the VP was smooth and uniform (Fig. 5b). Thanks to the knowledge of the current thickness of the CZ as indicated by the orange color, one can calculate the water content of the wet part of the sample, which otherwise would not be possible (Fig. 6; for further details see Tables 3 and 4 in Suppl. mat.). Therefore, uranine visualization of the VP is effective even in materials where the VP has an intricate geometry (e.g., heterogeneous materials, fractured zones, materials with hydrophobic portions, etc.).

The concentration of uranine in all the previously described experiments was between 1.3 and 3.0 g/l, depending on the color of the porous material used. Ideally, the concentration should be kept low, because of the possible clogging of pores by precipitated dye. However, it needs to be high enough so that its yellow color will be detectable on the material.

3.2. Comparison of uranine and BB solutions

We injected BB solution into the bottom of the glass containers filled with dry sand and allowed the material to become wet. At a certain level, as the solution was moving upwards, it started to evaporate. Subsequently, we compared BB's behavior with the behavior of uranine. Despite performed under the same conditions (the amounts of solutions injected, the sand used, and the same experimental procedures including limited packing of the material), the height of the colored zones was not identical: uranine colored the sand up to 8 cm in high, while BB only up to 7.5 cm high over the same time period (Fig. 7). More importantly, we observed that BB does not exactly visualize the wetting front, as wet parts were visually detectable above the BB line, unlike with uranine. Similar behaviors have been reported by several studies that used BB as a tracer where the dye patterns did not exactly match the wetting front during infiltration (Flury and Flühler, 1995; Devitt and Smith, 2002; Kasteel et al., 2002). This can be explained by stronger retardation of the BB. Therefore, even though BB can be successfully used as a tracer in evaporation drying experiments (when the material is saturated and let to dry, i.e. when the VP is receding), it is not always able to indicate the current wetting front and VP.

3.3. Experiments with uranine powder

Uranine can be used in the form of a dry red powder to visualize the DSL and CZ. After dusting it onto the surface of a porous material with the DSL and CZ present, two different color zones can be recognized: (1) a dark-orange zone, and (2) a red color zone (Fig. 8). The dark-orange zone (1) is the result of dissolution of the originally dry red powder into pore water; and the red color zone (2) indicates that no dissolution of the dry red powder occurs, as the material remains dry in this area (Fig. 8a, b). Therefore, the spatial distribution of the colors describes the spatial distribution of moisture within the porous media: the dark-orange zone represents the CZ, whereas the red color zone represents the DSL.

Unlike the uranine solution application, dusting with uranine powder does not explicitly highlight the VP. The VP can only be assumed at the border between the two differently colored parts (Fig. 8a, b), representing the CZ and DSL. Unlike with the use of uranine solution, the powder visualizes a single time frame, and therefore does not allow one to study the moisture system's history. Thus, it is not possible to distinguish whether the VP is retreating, or if it is progressing towards the surface. In fact, there might be no VP at all in the case that the wetting front is progressing, or when there is a lack of potential evaporation at the surface.

The change in color due to dissolution took 2–5 min, according to the moisture content and/or the thickness of the powder layer applied. For the correct use of the uranine powder dusting method, the spread of the powder must be uniform to reach quite a constant thickness; otherwise, there is a risk that the powder will not dissolve uniformly, and thus an apparent (but false) dry area will be observed (Fig. 8c).

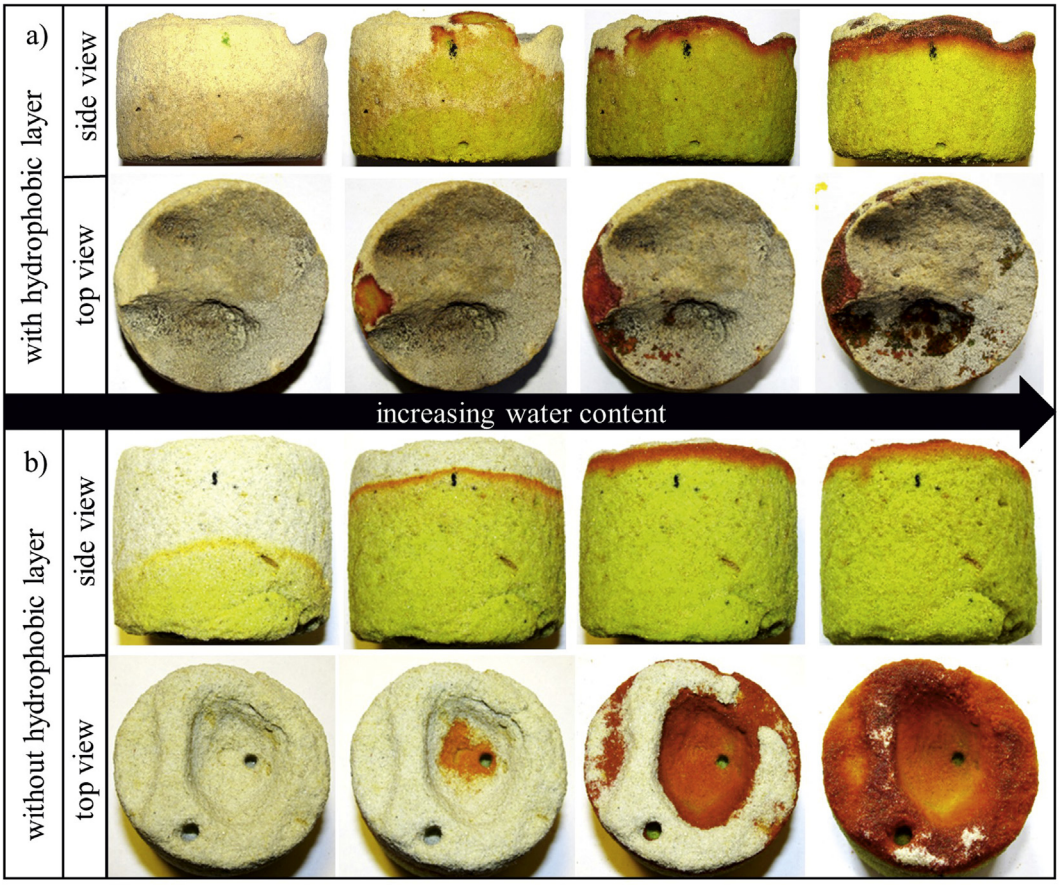

Fig. 5. The sandstone cores continuously fed by uranine solution from the bottom with an evaporating surface at the top. a) The sandstone core with several mm thick hydrophobic crust (exp. 1e), where the VP has a warped/uneven shape, as demonstrated by uranine visualization. b) The bare sandstone core (exp. 1b), where a smooth VP was created. For detailed data on the 1e exp. see Tables 3 and 4 in the Suppl. mat.

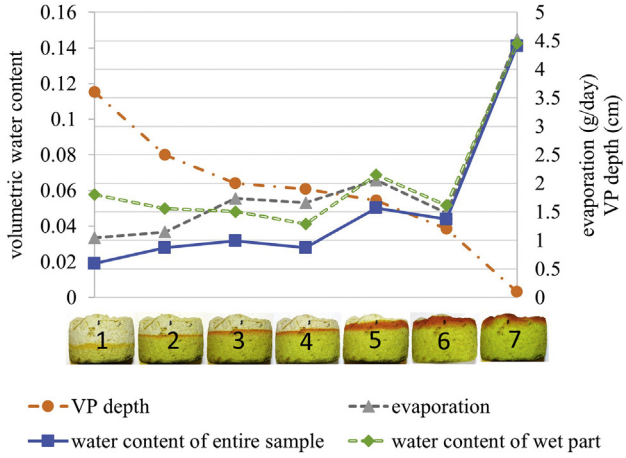

Fig. 6. A graph of the measured properties of the sandstone core in exp. 1e: The VP depth below the upper surface, evaporation, bulk water content, and calculated water content of the wet part due to knowledge of the CZ's thickness (for detailed values see Table 3 in the Suppl. mat.).

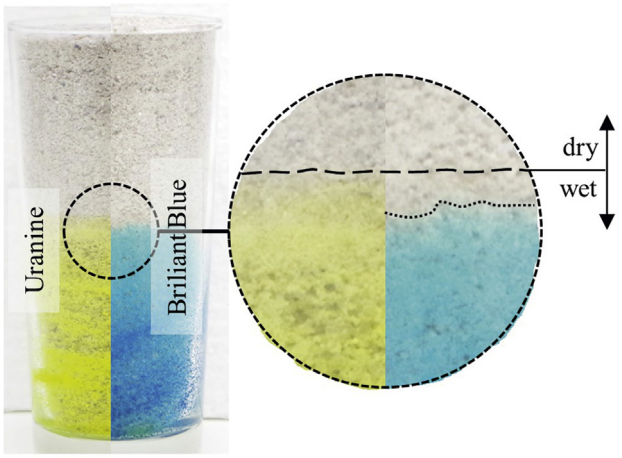

Fig. 7. Capillary uptake of uranine and BB under identical conditions (exp. 2). In the case of BB, unlike for uranine, a wet zone above the colored zone was observed.

3.4. Method utilization and comparison with other methods

In the laboratory, the use of uranine is applicable in almost any conceivable flow and evaporation experiments. The decision whether to use it in the solution or powder form depends on the purpose of the experiment. The advantage of using a solution is its ability to visualize the flow history, as the dye is already present in the transported liquid and zones' locations changes can be photo-documented repeatedly for long time periods. In addition to that, if the solution transport throughout the media is well photo-documented, the water flow velocity is easily computable, and any possible preferential flow can be detected. This utilization is based on the properties that uranine has in common with other dyes used in the vadose zone (e.g., BB, Rhodamine B, or Pyranine) (Flury and Wai, 2003; Gaspar, 1987; Wilson et al., 2016). We would like to underscore the use of uranine dye solution for

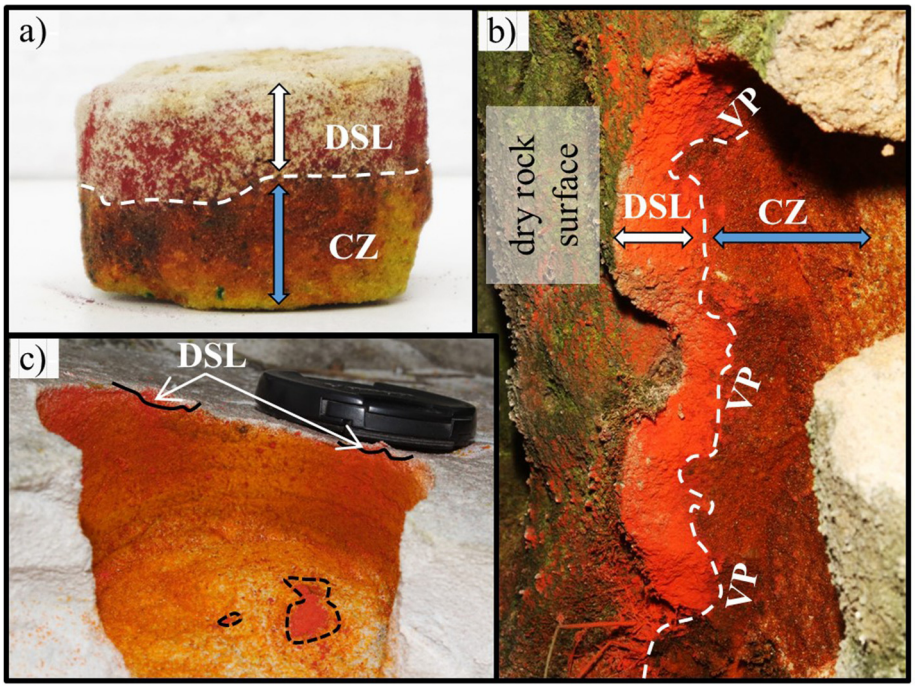

Fig. 8. The red dry uranine powder was dusted at the surface of a porous media. In couple of minutes (2–5), the powder dissolved in wet parts of the environment. Examples: a) The sandstone core which absorbed distilled water, was subsequently dusted by red dry uranine powder (exp. 3a). The wet area changed its color to dark-orange, but the dry part remained red. b) Uranine powder dusted into a freshly drilled hole in a sandstone surface (exp. 3b). Clear zoning of DSL (in the shallow subsurface) and CZ (in the deeper part of the body) is observable. The VP creates a border between the DSL and CZ. c) When the powder is not applied uniformly, apparent dry areas are formed where the uranine dust is too thick (in the picture highlighted by black dashed delimited areas). (For interpretation of the references to color in this figure legend, the reader is referred to the web version of this article.)

visualization of evaporation, and its ability to rapidly reflect the dynamics of the water system. However, there are cases when it is not convenient or advisable to use uranine solution. Perhaps the most significant disadvantage of the use of uranine solution is in the study of evaporation in the field, which has limited applicability. As the solution needs to be added to the environment, this changes the hydraulic field, and is also demanding of time as the evaporation processes might be relatively slow. Other drawbacks of using solution are the possible clogging of the pores, and possible density changes due to different concentrations of the original liquid in the pore space and injected into the solution. Another disadvantage of uranine application is its property to photodegrade (Käss, 1998; Gaigalas et al., 2004); with a photodecomposition decay coefficient $k = 9.5 \times 10^{-2}$–3.9×10^{-1} under sunny conditions (dimensionless, for details see review by Smart and Laidlaw, 1977). Therefore, it is essential to prevent or minimize the exposure of uranine to light during experiments.

The use of the powder can overcome some of the drawbacks of using uranine solution, as it can be applied without altering the hydraulic field, and its use is relatively quick. When the powder is used, it is sufficient to dust it onto the surface, and within minutes the color zones are displayed. The use of powder is especially practical in the field, where it can effectively visualize the DSL and CZ. However, repeated use of uranine powder is not possible *in situ* in drilled or burrowed holes if the holes are not sealed by a material with similar properties between readings, because the open hole affects the evaporation rate, and therefore repeated readings of the VP depth would be different from ambient conditions.

We suggest using uranine dye on all ranges of evaporation experiments from the mm to m scale. Uranine solution can be especially practical to use in wetting evaporation experiments, as it indicates the current wetting front and forms a distinctive visualization of the VP. The use of uranine solution to visualize preferential pathways in the field is a well-known and widespread practice (Wilson et al., 2016). However, we are not aware of any study using uranine to visualize subsurface evaporation from cracks or other preferential pathways. We believe that the use of uranine offers a simple method for such studies, and possibly enables differentiation between evaporation and transpiration, as plant roots uptake the uranine solution (Palmquist, 1939), and thus not causing a higher concentration of uranine in the soil. The powder use can find applications in studies focused on near sub-surface water movements in rock outcrops, buildings and sculptures made of porous rocks.

When we compare the use of uranine to visualize sub-surface evaporation dynamics with other methods, we find that even though they are often more precise, they are also more expensive and not so easily accessible (for details see Table 1 in Suppl. mat.). This is the case for nuclear magnetic resonance, X-ray tomography, neutron radiography, confocal microscopy, and gamma-ray densitometry. These methods are also not possible to use effectively in the field. Easily employable and inexpensive methods such as the electrical resistivity tomography, the heat-based methods, and tensiometry are less precise. Overall, in comparison with other methods, the use of uranine dye is both an easy-to-use and cost-effective (~140 USD per kg) method, with a fair resolution. Note that the electrical resistivity tomography at this research stage remains to be the only inexpensive and non-destructive method which is relevant when working on heritage sites or protected areas of rock outcrops (Mol and Viles, 2013).

3.5. Need for future development

When using uranine to visualize evaporation, one can only observe a 2D view of the moisture distribution at the surface; in order to gain knowledge about the insides of the material, destructive approach (digging/drilling/excavation) is needed (for both the solution and the powder methods; Figs. 4 and 8b, c). This hinders the wider use of uranine in studying moisture at protected natural rock outcrops, or in building structures and statues where any destructive approach is not acceptable. Here, we presented the visualization of the VP in the 80 mm wide burrowed/drilled holes, and so far, we are limited by the hole being sufficiently wide to ensure a clear view of the line between the CZ and DSL. Therefore, significant progress in miniaturization of this invasive method is needed.

Concerning the use of uranine solution, we observed that if the VP is fixed for a relatively long time, precipitation of uranine occurs. Even though we did not observe any role of this clogging upon the evaporation rate, we believe that more research is needed to quantify this in relationship to the water flow dynamics. Here, we have presented experiments conducted in porous materials with the porosity of sand,

and thus another area that requires further research is the use of uranine in evaporation studies within materials of different pore sizes such as clays or gravels. Additionally, we suggest conducting more research on the role of uranine solution concentration on evaporation rates, as well as a study comparing the use of uranine to other commonly used dyes not mentioned in this paper (such as Rhodamine B or Pyranine).

4. Conclusion

This paper has presented several examples where uranine dye was used to visualize the vaporization plane, capillary zone, and the dry surface layer. The uranine solution visualizes the vaporization plane by forming a distinctive dark-orange zone caused by evaporation of the pore water, and hence increased uranine concentration. The use of uranine also enables one to distinguish the zones of vapor and capillary flow, thanks either to the visualization of the vaporization plane by the uranine solution, or by application of the uranine powder on porous materials. When compared to the Brilliant Blue dye, uranine solution has lower retardation and better visualizes both the capillary zone and the vaporization plane; thus, it should be the dye of choice for all kinds of evaporation experiments. Uranine dye can find use in various laboratory evaporation experiments and field studies of sub-surface evaporation, from both soil and rock outcrops. Even though this method is destructive in compact materials, if miniaturized, it might be used to detect the vaporization plane and the salt enriched zone in cultural heritage sites. Overall, the presented technique is accurate, cost-effective, and straightforward in its use.

Acknowledgements

This research was funded by the Czech Science Foundation [GA16-19459S] and Charles University Grant Agency [GAUK #1046217] and supported by Center for Geosphere Dynamics [UNCE/SCI/006]. We thank Dr. Lisa Mol, two other anonymous reviewers and the associate editor Juan V Giraldez who significantly helped to improve this article.

Declaration of interest

None.

Contributions

TW and MS designed and conducted most of the experiments, JB first observed the phenomenon of VP visualization and contributed by the design of some pilot and field experiments. TW and MS wrote most of the manuscript, JB participated in the manuscript writing and with critical comments and advice.

Appendix A. Supplementary data

Supplementary data associated with this article can be found, in the online version, at https://doi.org/10.1016/j.jhydrol.2018.08.028.

References

Appelo, C.A.J., Postma, D., 2013. Geochemistry, Groundwater and Pollution. CRC Press, Boca Raton.
Bittelli, M., Ventura, F., Campbell, G.S., Snyder, R.L., Gallegati, F., Pisa, P.R., 2008. Coupling of heat, water vapor, and liquid water fluxes to compute evaporation in bare soils. J. Hydrol. 362, 191–205. https://doi.org/10.1016/j.jhydrol.2008.08.014.
Bruthans, J., Filippi, M., Slavík, M., Svobodová, E., 2018. Origin of honeycombs: testing the hydraulic and case hardening hypotheses. Geomorphology 303, 68–83. https://doi.org/10.1016/j.geomorph.2017.11.013.
Budowle, B., Leggitt, J.L., Defenbaugh, D.A., Keys, K.M., Malkiewicz, S.F., 2000. the presumptive reagent fluorescein for detection of dilute bloodstains and subsequent STR typing of recovered DNA. J. Forensic Sci. 45. https://doi.org/10.1520/jfs14835j.
Canadian Medical Association Journal, 1959. New Drugs. 80 (12), 997–998.
Colour Index, 2001. Colour Index International Fourth Edition Online. Society of Dyers and Colourists and the American Asso ciation of Textile Chemists and Colorists, http://www.colourindex.org, accessed September 2004, Bradford, England.
Daily, W., Ramirez, A., LaBrecque, D., Nitao, J., 1992. Electrical resistivity tomography of vadose water movement. Water Resour. Res. 28, 1429–1442. https://doi.org/10.1029/91WR03087.
Deinert, M.R., Parlange, J.Y., Steenhuis, T., Throop, J., Ünlü, K., Cady, K.B., 2004. Measurement of fluid contents and wetting front profiles by real-time neutron radiography. J. Hydrol. 290, 192–201. https://doi.org/10.1016/j.jhydrol.2003.11.018.
Devitt, D.A., Smith, S.D., 2002. Root channel macropores enhance downward movement of water in a Mojave Desert ecosystem. J. Arid Environ. 50, 99–108. https://doi.org/10.1006/jare.2001.0853.
Falchi, L., Zendri, E., Müller, U., Fontana, P., 2015. The influence of water-repellent admixtures on the behaviour and the effectiveness of Portland limestone cement mortars. Cem. Concr. Compos. 59, 107–118. https://doi.org/10.1016/j.cemconcomp.2015.02.004.
Fidríková, D., Greif, V., Dieška, P., Štofanik, V., Kubičár, L., Vlčko, J., 2013. Monitoring of the temperature–moisture regime in St. Martin's Cathedral tower in Bratislava. Environ. Earth Sci. 69, 1481–1489. https://doi.org/10.1007/s12665-012-2160-7.
Flury, M., Flühler, H., 1995. Tracer characteristics of brilliant blue FCF. Soil Sci. Soc. Am. J. 59, 22. https://doi.org/10.2136/sssaj1995.03615995005900010003x.
Flury, M., Wai, N.N., 2003. Dyes as tracers for vadose zone hydrology. Rev. Geophys. 41, 1002. https://doi.org/10.1029/2001RG000109.
Gaigalas, A.K., Wang, L., Cole, K.D., Humphries, E., 2004. Photodegradation of fluorescein in solutions containingn-propyl gallate. J. Phys. Chem. A 108, 4378–4384. https://doi.org/10.1021/jp0371377.
Gaspar, E., 1987. Modern Trends in Tracer Hydrology. CRC Press, Boca Raton, FL.
Germán-Heins, J., Flury, M., 2000. Sorption of Brilliant Blue FCF in soils as affected by pH and ionic strength. Geoderma 97, 87–101. https://doi.org/10.1016/s0016-7061(00)00027-6.
Gerke, K.M., Sidle, R.C., Tokuda, Y., 2008. Sorption of Uranine on Forest Soils. Hydrol. Res. Lett. 2, 32–35. https://doi.org/10.3178/hrl.2.32.
Gerke, K.M., Sidle, R.C., Mallants, D., 2013. Criteria for selecting fluorescent dye tracers for soil hydrological applications using Uranine as an example. J. Hydrol. Hydromech. 61, 313–325. https://doi.org/10.2478/johh-2013-0040.
Gerke, K.M., Sidle, R.C., Mallants, D., 2015. Preferential flow mechanisms identified from staining experiments in forested hillslopes. Hydrol. Process. 29 (21), 4562–4578. https://doi.org/10.1002/hyp.10468.
Grapsas, N., Shokri, N., 2014. Acoustic characteristics of fluid interface displacement in drying porous media. Int. J. Multiph. Flow 62, 30–36. https://doi.org/10.1016/j.ijmultiphaseflow.2014.01.011.
Gupta, L.N., 1974. An approximate solution of the generalized Stefan's problem in a porous medium. Int. J. Heat Mass Transf. 17, 313–321. https://doi.org/10.1016/0017-9310(74)90092-1.
Hillel, D., 2004. Introduction to Environmental Soil Physics. Elsevier Academic Press, Amsterdam.
Huinink, H.P., Pel, L., Kopinga, K., 2004. Simulating the growth of tafoni. Earth Surf. Process. Landforms 29, 1225–1233. https://doi.org/10.1002/esp.1087.
Idso, S.B., Reginato, R.J., Jackson, R.D., Kimball, B.A., Nakayama, F.S., 1974. The three stages of drying of a field soil1. Soil Sci. Soc. Am. J. 38, 831. https://doi.org/10.2136/sssaj1974.03615995003800050037x.
Kasnavia, T., Vu, D., Sabatini, D.A., 1999. Fluorescent dye and media properties affecting sorption and tracer selection. Ground Water 37, 376–381. https://doi.org/10.1111/j.1745-6584.1999.tb01114.x.
Käss, W., 1998. Tracing Technique in Geohydrology. Balkema, Rotterdam (581 p).
Kasteel, R., Vogel, H.J., Roth, K., 2002. Effect of non-linear adsorption on the transport behaviour of Brilliant Blue in a field soil. Eur. J. Soil Sci. 53, 231–240. https://doi.org/10.1046/j.1365-2389.2002.00437.x.
Ketelsen, H., Meyer-Windel, S., 1999. Adsorption of brilliant blue FCF by soils. Geoderma 90, 131–145. https://doi.org/10.1016/s0016-7061(98)00119-0.
Kurtzman, D., Baram, S., Dahan, O., 2016. Soil – Aquifer phenomena affecting groundwater under vertisols: a review. Hydrol. Earth Syst. Sci. 20, 1–12. https://doi.org/10.5194/hess-20-1-2016.
Lakowicz, J.R., 2006. Principles of Fluorescence Spectroscopy. Springer, New York, NY.
Lehmann, P., Or, D., 2009. Evaporation and capillary coupling across vertical textural contrasts in porous media. Phys. Rev. E 80, 46318. https://doi.org/10.1103/PhysRevE.80.046318.
Lehoux, A.P., Rodts, S., Faure, P., Michel, E., Courtier-Murias, D., Coussot, P., 2016. Magnetic resonance imaging measurements evidence weak dispersion in homogeneous porous media. Phys. Rev. E 94. https://doi.org/10.1103/physreve.94.053107.
Mathew, T., Kundan, S., Abdulsamad, M.I., Menon, S., Dharan, B.S., Jayakumar, K., 2014. Multiple muscular ventricular septal defects: use of fluorescein dye to identify residual defects. Ann. Thor. Surg. 97. https://doi.org/10.1016/j.athoracsur.2013.10.059.
McAllister, D., Warke, P., McCabe, S., Gomez-Heras, M., 2016. Evaporative moisture loss from heterogeneous stone: Material-environment interactions during drying. Geomorphology 273, 308–322. https://doi.org/10.1016/j.geomorph.2016.08.008.
Marmion, D.M., 1991. Handbook of US Colorants: Foods, Drugs, Cosmetics, and Medical Devices. Wiley, New York.
Mikhailov, M.D., 1975. Exact solution of temperature and moisture distributions in a porous half-space with moving evaporation front. Int. J. Heat Mass Transf. 18, 797–804. https://doi.org/10.1016/0017-9310(75)90209-4.
Mol, L., Viles, H.A., 2010. Geoelectric investigations into sandstone moisture regimes: implications for rock weathering and the deterioration of San Rock Art in the Golden

Gate Reserve, South Africa. Geomorphology 118, 280–287. https://doi.org/10.1016/j.geomorph.2010.01.008.
Mol, L., Viles, H., 2013. Exposing drying patterns: using electrical resistivity tomography to monitor capillary rise in sandstone under varying drying conditions. Environ. Earth Sci. 68, 1647–1659. https://doi.org/10.1007/s12665-012-1858-x.
Mon, J., Flury, M., Harsh, J.B., 2006. Sorption of four triarylmethane dyes in a sandy soil determined by batch and column experiments. Geoderma 133, 217–224. https://doi.org/10.1016/j.geoderma.2005.07.008.
Morris, C., Mooney, S., Young, S., 2008. Sorption and desorption characteristics of the dye tracer, Brilliant Blue FCF, in sandy and clay soils. Geoderma 146, 434–438. https://doi.org/10.1016/j.geoderma.2008.06.021.
Noga, E.J., Udomkusonsri, P., 2002. Fluorescein: a rapid, sensitive, nonlethal method for detecting skin ulceration in fish. Vet. Pathol. 39, 726–731. https://doi.org/10.1354/vp.39-6-726.
Or, D., Lehmann, P., Shahraeeni, E., Shokri, N., 2013. Advances in soil evaporation physics—a review. Vadose Zo. J. 12. https://doi.org/10.2136/vzj2012.0163.
Palmquist, E.M., 1939. The path of fluorescein movement in the kidney bean, phaseolus vulgaris. Am. J. Bot. 26, 665–667. https://doi.org/10.1002/j.1537-2197.1939.tb09332.x.
Rad, M.N., Shokri, N., Keshmiri, A., Withers, P.J., 2015. Effects of grain and pore size on salt precipitation during evaporation from porous media. Transp. Porous Media 110, 281–294. https://doi.org/10.1007/s11242-015-0515-8.
Reis, N., Griffiths, R., Mantle, M., Gladden, L., 2003. Investigation of the evaporation of embedded liquid droplets from porous surfaces using magnetic resonance imaging. Int. J. Heat Mass Transf. 46, 1279–1292. https://doi.org/10.1016/s0017-9310(02)00395-2.
Richards, L.A., 1931. Capillary conduction of liquids through porous mediums. Physics 1, 318–333. https://doi.org/10.1063/1.1745010.
Rijniers, L.A., Huinink, H.P., Pel, L., Kopinga, K., 2005. Experimental evidence of crystallization pressure inside porous media. Phys. Rev. Lett. 94. https://doi.org/10.1103/physrevlett.94.075503.
Sacha, J., Jelinkova, V., Snehota, M., Vontobel, P., Hovind, J., Cislerova, M., 2015. Water and air redistribution within a dual permeability porous system investigated using neutron imaging. Phys. Proc. 69, 530–536. https://doi.org/10.1016/j.phpro.2015.07.075.
Sabatini, D.A., 2000. Sorption and intraparticle diffusion of fluorescent dyes with consolidated aquifer media. Ground Water 38, 651–656. https://doi.org/10.1111/j.1745-6584.2000.tb02700.x.
Sabatini, D.A., Austin, T.A., 1991. Characteristics of rhodamine WT and fluorescein as adsorbing ground-water tracers. Ground Water 29, 341–349. https://doi.org/10.1111/j.1745-6584.1991.tb00524.x.
Slavík, M., Bruthans, J., Filippi, M., Schweigstillová, J., Falteisek, L., Řihošek, J., 2017. Biologically-initiated rock crust on sandstone: Mechanical and hydraulic properties and resistance to erosion. Geomorphology 278, 298–313. https://doi.org/10.1016/j.geomorph.2016.09.040.
Smart, P.L., Laidlaw, I.M.S., 1977. An evaluation of some fluorescent dyes for water tracing. Water Resour. Res. 13, 15–33. https://doi.org/10.1029/wr013i001p00015.
Sněhota, M., Císlerová, M., Gao Amin, M.H., Hall, L.D., 2010. Tracing the entrapped air in heterogeneous soil by means of magnetic resonance imaging. Vadose Zo. J. 9, 373–384. https://doi.org/10.2136/vzj2009.0103.
Shahidzadeh-Bonn, N., Azouni, A., Coussot, P., 2007. Effect of wetting properties on the kinetics of drying of porous media. J. Phys. Condens. Matter 19. https://doi.org/10.1088/0953-8984/19/11/112101.
Shokri, N., Lehmann, P., Or, D., 2009. Critical evaluation of enhancement factors for vapor transport through unsaturated porous media. Water Resour. Res. 45, 1–9. https://doi.org/10.1029/2009WR007769.
Shokri, N., Or, D., 2011. What determines drying rates at the onset of diffusion controlled stage-2 evaporation from porous media? Water Resour. Res. 47. https://doi.org/10.1029/2010wr010284.
Topp, G.C., Davis, J.L., Annan, A.P., 1982. Electromagnetic determination of soil water content using TDR: I. Applications to wetting fronts and steep gradients1. Soil Sci. Soc. Am. J. 46, 672. https://doi.org/10.2136/sssaj1982.03615995004600040002x.
Trautz, A.C., Smits, K.M., Schulte, P., Illangasekare, T.H., 2014. Sensible heat balance and heat-pulse method applicability to in situ soil-water evaporation. Vadose Zo. J. 13. https://doi.org/10.2136/vzj2012.0215.
Viitanen, H., Vinha, J., Salminen, K., Ojanen, T., Peuhkuri, R., Paajanen, L., Lähdesmäki, K., 2010. Moisture and bio-deterioration risk of building materials and structures. J. Build. Phys. 33, 201–224. https://doi.org/10.1177/1744259109343511.
Vlček, L., Falátková, K., Schneider, P., 2017. Identification of runoff formation with two dyes in a mid-latitude mountain headwater. Hydrol. Earth Syst. Sci. 21 (6), 3025. https://doi.org/10.5194/hess-21-3025-2017.
Wilson, G.V., Rigby, J.R., Ursic, M., Dabney, S.M., 2016. Soil pipe flow tracer experiments: 1 Connectivity and transport characteristics. Hydrol. Process. 30, 1265–1279. https://doi.org/10.1002/hyp.10713.
Xiao, Z., Lu, S., Heitman, J., Horton, R., Ren, T., 2012. Measuring subsurface soil-water evaporation with an improved heat-pulse probe. Soil Sci. Soc. Am. J. 76, 876. https://doi.org/10.2136/sssaj2011.0052n.
Xu, L., Davies, S., Schofield, A.B., Weitz, D.A., 2008. Dynamics of drying in 3D porous media. Phys. Rev. Lett. 101, 29–32. https://doi.org/10.1103/PhysRevLett. 101.094502.